AFRL-RV-PS-
TR-2022-0066

AFRL-RV-PS-
TR-2022-0066

STUDY OF RADIATION-HARD CdTe/MgCdTe DOUBLE-HETEROSTRUCTURE THIN-FILM SOLAR CELLS USING A NOVEL LIFTOFF TECHNOLOGY

Yong-Hang Zhang

Arizona State University
975 S. Myrtle Ave.
Tempe, AZ 85287

6 Oct 2021

Final Report

APPROVED FOR PUBLIC RELEASE; DISTRIBUTION IS UNLIMITED.

AIR FORCE RESEARCH LABORATORY
Space Vehicles Directorate
3550 Aberdeen Ave SE
AIR FORCE MATERIEL COMMAND
KIRTLAND AIR FORCE BASE, NM 87117-5776

NOTICE AND SIGNATURE PAGE

AFRL-RV-PS-TR-2022-0066 HAS BEEN REVIEWED AND IS APPROVED FOR PUBLICATION IN ACCORDANCE WITH ASSIGNED DISTRIBUTION STATEMENT.

//SIGNED//

PRESTON WEBSTER
Program Manager

//SIGNED//

Tech Advisor, Space Control Technologies Branch

//SIGNED//

JOHN BEAUCHEMIN
Chief Engineer, Spacecraft Technology Division
Space Vehicles Directorate

Report Documentation Page

Form Approved
OMB No. 0704-0188

1. REPORT DATE *(DD-MM-YYYY)*
06-10-2021

2. REPORT TYPE
Final Report

3. DATES COVERED *(From - To)*
06-Jan-2020 06-Oct-2021

4. TITLE AND SUBTITLE
Study of Radiation-Hard CdTe/MgCdTe Double-Heterostructure Thin-Film Solar Cells Using a Novel Liftoff Technology

5a. CONTRACT NUMBER
FA9453-20-2-0011

5b. GRANT NUMBER

5c. PROGRAM ELEMENT NUMBER C6601F

5d. PROJECT NUMBER
4846

5e. TASK NUMBER

5f. WORK UNIT NUMBER V1SG

6. AUTHOR(S)

Yong-Hang Zhang

7. PERFORMING ORGANIZATION NAME(S) AND ADDRESS(ES)

Arizona State University
975 S. Myrtle Ave.
Tempe, AZ 85287

8. PERFORMING ORGANIZATION REPORT NUMBER

9. SPONSORING / MONITORING AGENCY NAME(S) AND ADDRESS(ES)
Air Force Research Laboratory
Space Vehicles Directorate
3550 Aberdeen Ave SE
Kirtland AFB, NM 87117-5776

10. SPONSOR/MONITOR'S ACRONYM(S)
AFRL/RVSU

11. SPONSOR/MONITOR'S REPORT NUMBER(S)
AFRL-RV-PS-TR-2022-0066

12. DISTRIBUTION / AVAILABILITY STATEMENT
Approved for public release; distribution is unlimited.

13. SUPPLEMENTARY NOTES
Study of Radiation-Hard CdTe/MgCdTe Double-Heterostructure Thin-Film Solar Cells Using a Novel Liftoff Technology

14. ABSTRACT
In collaboration with AFRL Space Vehicles and Direct Energy Directorates, the objective of this proposal is to

- Optimize the novel lift-off technology using water-soluble MgTe sacrificial layer grown on lattice matched InSb substrate for light-weight and low-cost solar cells and photodetector applications-• Demonstrate the study of radiation tolerant thin-film CdTe/MgCdTe doubleheterostructures and solar cells using the water-soluble lift-off technology
- Demonstrate wafer-transfer thin-film CdTe/InSb two-color photodetectors and study their radiation tolerance under proton bombardment

15. SUBJECT TERMS
CdTe, solar OR photovoltaic, liftoff OR substrate removal, radiation hardness OR radiation tolerance

16. SECURITY CLASSIFICATION OF:			17. LIMITATION OF ABSTRACT	18. NUMBER OF PAGES	19a. NAME OF RESPONSIBLE PERSON
a. REPORT	**b. ABSTRACT**	**c. THIS PAGE**			Preston Webster
Unclassified	Unclassified	Unclassified	Unlimited	24	**19b. TELEPHONE NUMBER** *(include area code)*

(This Page Intentionally Left Blank)

TABLE OF CONTENTS

LIST OF FIGURES

Page

LIST OF TABLES

(This Page Intentionally Left Blank)

1.0 SUMMARY

Recently a new Epitaxial Lift-Off (ELO) method for monocrystalline CdTe thin films was reported using MgTe as a sacrificial layer [1-3]. High-quality CdTe/MgCdTe double heterostructures (DH) and MgTe can be grown on nearly-lattice-matched InSb substrates by using molecular-beam epitaxy (MBE). The MgTe sacrificial layer is water soluble, while both the DH and the substrate have extremely low etching rates in deionized (DI) water. Therefore this ELO method is a promising method to lift-off high quality monocrystalline DH thin films. Since only water is used during the ELO process, the substrate is intact and can be reused almost indefinitely without the need for re-polishing. Furthermore, the wide-bandgap MgCdTe barriers serve as carrier selective barriers and passivation layers to the CdTe absorber. The lift-off MgCdTe surface is therefore expected to have little impact on the effective minority carrier lifetime of the CdTe DH [4]. A back reflective mirror can be added to enhance the light extraction and photon-recycling effect, reducing the necessary absorber thickness to approximately half its original value. This leads to decreased total SRH recombination current density and increased open-circuit voltage (V_{OC}) with nearly the same short-circuit current density (J_{SC}). A similar approach has successfully demonstrated thin-film GaAs solar cells with a record efficiency of 29.1% [5]. Kapton tape attached to the top surface of the sample was used in previous study of MgTe-based ELO [3]. Submersion of the sample in DI water dissolved the MgTe layer and the thin film was lifted off with the tape. Although the lift-off process was successful, the Kapton tape is not an ideal superstrate since the flexible tape makes the thin film susceptible to wrinkles and defects during the ELO process, reducing photoluminescence (PL) intensity in the center area and broadening the CdTe peak in the X-ray diffraction (XRD) pattern. The strong PL signal observed at the edge of the lifted-off thin film is attributed to luminescence concentration as the film acts as an efficient waveguide. In this work, hard-baked photoresist is used as the superstrate to rigidly support the thin film during the ELO process. Additionally, this superstrate supplies the necessary surface tension that enables the reaction products of the thin MgTe with DI water to diffuse out from the etching fronts and let the etching continue.

2.0 INTRODUCTION

Flexible thin-film solar cells with high power density and specific power are highly desirable for both terrestrial and space applications. Epitaxial lift-off (ELO) technology, which enables the development of flexible thin-film solar cells, has been successfully demonstrated for III-V materials and ZnSe based II-VI semiconductors [6-8] using highly selective etchants and sacrificial layers. ELO has been demonstrated in thin film photovoltaics including polycrystalline CdTe and $CuIn_xGa_{1-x}Se_2$ (CIGS) solar cells using the sacrificial layer approach. Devices were lifted off from polyimide films by constructing a glass/NaCl/polyimide/CdTe (CIGS) stack and then dissolving the NaCl in water [9,10]. Another ELO method was demonstrated by depositing polycrystalline CdS/CdTe films on Si/SiO_2 substrate, resulting in a fast lift-off process in water [11]. The thin films can be delaminated automatically using these methods. However, their application is limited to polycrystalline systems due to the large lattice-mismatch between substrates or sacrificial layers and the epitaxial thin films. Alternatively, several mechanical and thermomechanical lift-off methods have been reported, such as delaminating CIGS films on a Mo layer and lift-off of CdTe films by thermally shocking a polymeric stressor layer in liquid nitrogen [12-14]. Although these methods demonstrated novel approaches to delaminate high-quality polycrystalline thin films, successful ELO of high-quality monocrystalline CdTe devices has not been reported.

3.0 METHODS, ASSUMPTIONS, AND PROCUDURES

3.1 Epitaxial lift-off technology for monocrystalline CdTe thin films

The basic process of MgTe-based ELO is depicted in Figure 1. Each sample is coated with photoresist upon removal from the MBE growth chamber and then moved to a hot plate for hard bake. Several layers of photoresist are coated to achieve appropriate amount of tension. The sample

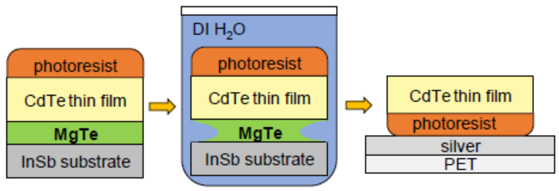

Figure 1. Schematic ELO Process of CdTe/MgCdTe DH Using Photoresist as the Superstrate

is then immersed in DI water. MgTe is dissociated and the CdTe thin film is lifted off with the photoresist. Typically, the process takes about 15 minutes to lift off a 1 cm × 1 cm thin film from the substrate in 55˚C DI water. The free-standing thin film is then transferred to a polyethylene terephthalate (PET) substrate coated with Ag as a reflective mirror. Future thin-film solar cell fabrication is planned using indium to bond the CdTe samples with conductive PET substrates prior to the lift-off process, [15] or to use an elastomer such as PDMS as the superstrate to lift off, transfer, and print the thin films [16, 17].

Fig. 2a shows the layer structure of a conventional CdTe/MgCdTe DH solar cell design which exhibits a record V_{OC} up to 1.11 V [18, 19]. The CdTe lift-off samples in this study are shown in Fig. 2b and are designed with a reversed layer sequence to be compatible with the MgTe sacrificial layer ELO process. Apart from the layer sequence, the changes of the new designs are i) the thickness of i-$Mg_{0.4}Cd_{0.6}Te$ barrier is increased from 15 nm to 20 nm to minimize electron tunneling and consequent p-contact/i-$Mg_{0.4}Cd_{0.6}Te$ interface recombination; [20, 21] ii) the thickness of n-$Mg_{0.24}Cd_{0.76}Te$ barrier is decreased from 50 nm to 20 nm to reduce the parasitic absorption due to light reflection from the back mirror; iii) two structures A and B feature different absorber thickness of 0.5 µm and 1 µm, respectively.

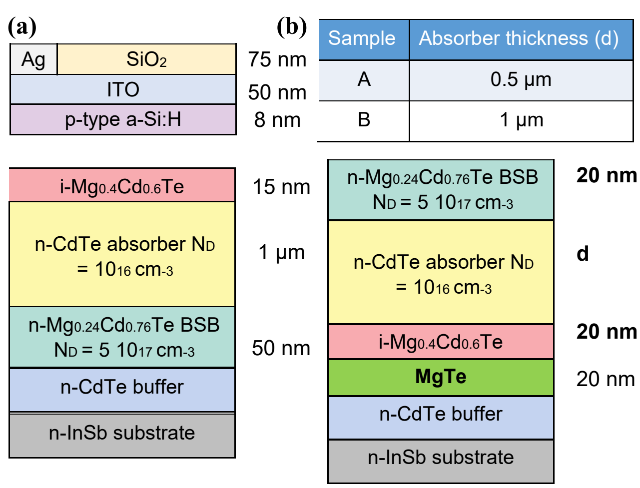

Figure 2. (a) Layer Structure of the Conventional CdTe/MgCdTe DH Solar Cells Design (b) Layer Structures of Newly Designed CdTe Lift-off Samples with MgTe Sacrificial Layers

X-ray diffraction was used to investigate the crystalline properties of the lift-off thin films before and after ELO. Pre-ELO (top) and post-ELO (bottom) coupled -2 XRD scans of the (004) plane for structure A are shown in Fig. 3. The post-ELO scan shows that both the MgTe peak at 29° and the InSb substrate peak are absent while the CdTe absorber peak and the features corresponding to the $Mg_{0.24}Cd_{0.76}Te$ and $Mg_{0.4}Cd_{0.6}Te$ barriers remain. Full width at half maximum (FWHM) of the CdTe absorber peak does not change significantly after the ELO. These findings indicate a successful ELO of the CdTe DH thin films with the assistance of photoresist.

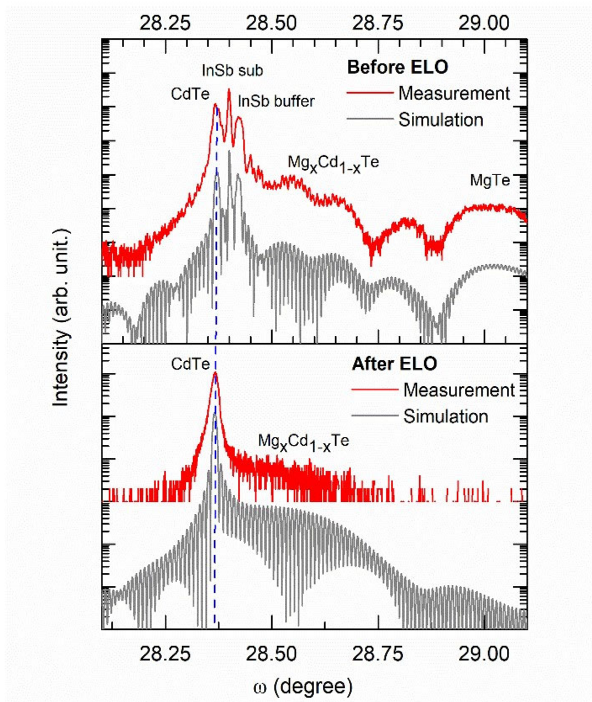

Fig. 3 Coupled ω-2θ Scans of the (004) Plane for (top) As-grown Sample A on an InSb(001) Substrate and (bottom) the Free-standing CdTe/MgCdTe DH Thin Film After ELO

The i-$Mg_{0.4}Cd_{0.6}Te$ layer, which passivates the CdTe absorber and serves as an electron blocking layer, is exposed to the air after ELO. This layer could possibly react with DI water due to its 40% Mg composition, which would lead to increased surface recombination and low optical performance in the thin film despite unchanged crystalline quality [20, 22]. Atomic force microscopy (AFM) is used to investigate the surface morphology of thin film structure B to confirm the i-$Mg_{0.4}Cd_{0.6}Te$ layer is intact after ELO. A 5 µm × 5 µm range image is shown in Fig. 4. The root mean square (RMS) roughness of 6.69 Å is similar to that obtained on an epitaxial layer surface, suggesting the extremely low etching rate of i-$Mg_{0.4}Cd_{0.6}Te$ in DI water.

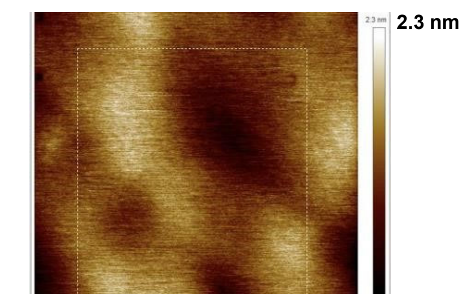

Fig. 4 AFM Image of i-$Mg_{0.4}Cd_{0.6}Te$ Surface Morphology of Post-ELO Thin Film with Structure B. Image Dimensions are 5 µm × 5 µm

The optical performance of the as-grown samples and post-ELO thin films is characterized by using room-temperature PL spectroscopy. The laser wavelength is 532 nm yielding a penetration depth in the CdTe absorber of less than 0.1 µm. Fig. 5a compares the PL of a conventional CdTe DH sample and the lift-off samples with structures A and B before ELO. The PL intensity of the lift-off samples is stronger than the conventional CdTe DH sample because the thicker i-$Mg_{0.4}Cd_{0.6}Te$ barrier further suppresses tunneling of the photogenerated carriers from the absorber to the surface to recombine non-radiatively [20, 21]. The structure A sample with 0.5 m thick absorber shows even higher PL intensity than the structure B sample with 1 m thick absorber due to a higher photogenerated carrier concentration and lower total SRH non-radiative recombination rate per unit area.

In Fig. 5b, stronger PL intensity is observed in the post-ELO films than those in the asgrown lift-off samples. This indicates the light extraction and photon-recycling effect of the CdTe thin films is enhanced by replacing the absorptive substrate with a reflective back mirror. Increased PL intensity is observed across the entire sample area of the post-ELO films.

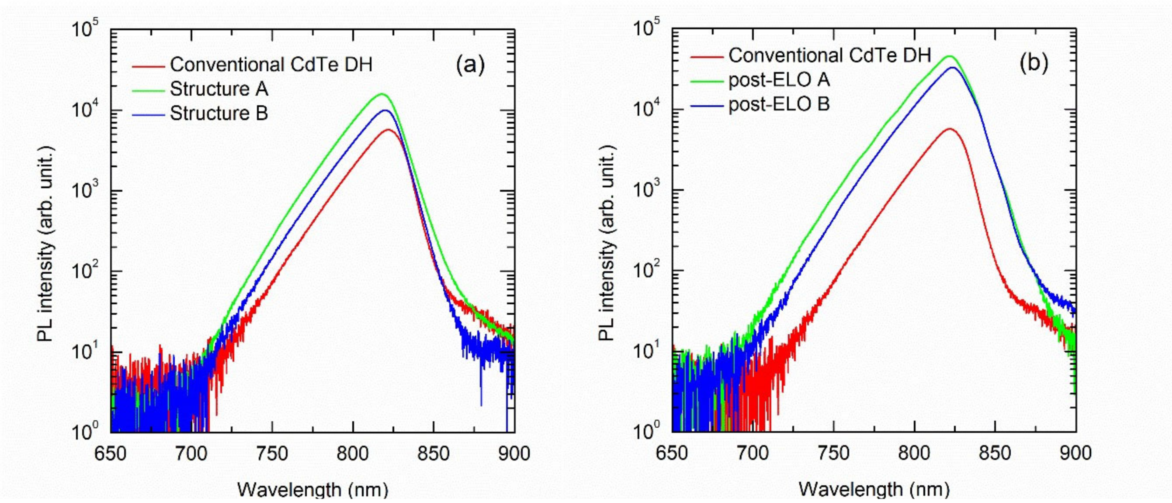

Figure 5. (a) PL Spectra from Conventional CdTe DH Sample and from As-grown CdTe Lift-off Samples with Structure A and B (b) PL Spectra from Conventional CdTe DH Sample and Free-standing Thin Films of Structure A and B with Ag Back Mirror

Photoluminescence quantum efficiency (PLQE) measurements are performed and the external luminescence quantum efficiency (η_{ext}) is measured. Details on the experimental procedure and theoretical analysis can be found in [23]. Using the formula [24, 25]

$$iV_{OC} = V_{OC,l} - kT\ |\ln\ (\eta_{ext})|\ /q$$

the implied open-circuit voltage (iV_{OC}) of a solar cell, or the quasi-fermi-level splitting in the absorber region, can be measured. η_{ext} is the ratio of photons that escape from the front surface to the electron-hole pairs generated in the solar cell absorber. $V_{OC,l}$ is the V_{OC} of a solar cell when the recombination is purely radiative, emittance to the back-surface is zero, and there is zero voltage loss due to carrier transport. The results are summarized in Table .

Table 1. Summary of PLQE Measurement Results. SC design represents conventional monocrystalline CdTe DH solar cell design. Measured open-circuit voltage V_{OC} is reported for the complete device described in [19]

Sample	η_{ext} at 1 sun	iV_{OC} (V)	V_{OC} (V)
SC design	1.54%	1.119	1.11 [19]
structure A	3.65%	1.141	-
structure B	1.80%	1.123	-
ELO A	5.35%	1.152	-
ELO B	3.39%	1.139	-

The optical absorption, or the number of carriers optically injected into the CdTe absorber, is one of the key factors in the calculation of iV_{OC}. The absorption differs for structures with smooth vs textured surfaces, absorptive vs reflective substrates, and differing refractive index. A total of 12 kinds of statistical ray tracing models are presented in the previous studies [26, 27] assuming the maximal scattering case with an angular Lambertian distribution. The absorption at the laser wavelength in the CdTe layer in the MBE grown samples and post-ELO thin films with smooth surfaces and interfaces can be accurately simulated by wave optics using the optical constants (refractive index, n, and extinction coefficient, k) and the thickness of each layer. The measured iV_{OC} of the conventional CdTe DH samples is in excellent agreement with the V_{OC} of the processed solar cells [19]. In the light absorption simulation of the ELO thin films above, however, the absorption of photoresist is ignored. This results in underestimation of the ELO film iV_{OC} values. Measurements of the ELO thin films with 0.5 μm thick absorber (ELO A) demonstrated a η_{ext} of 5.35% and an iV_{OC} of 1.152 V. The CdTe thin-film solar cells based on structure A could achieve a V_{OC} of 1.15 V or even higher by using the same processing flow of the conventional CdTe DH solar cells.

A thin-film solar cell with 0.5-μm-thick absorber would maintain a similar J_{SC} to the conventional CdTe DH solar cell design by incorporating a 150-nm-thick Ag layer as back mirror. Fig. 6 depicts the simulated absorption of the thin-film solar cells with a calculated photo-current density of 24.7 mA/cm^2 using wave optics. The simulated structure is SiO_2/ITO/a-Si:H/CdTe DH (structure A)/Ag/PET. By optimizing the p-contact to reduce the parasitic absorption, such as depositing a thinner a-Si:H layer with higher doping density or replacing the a-Si:H with a wider band gap material, the J_{SC} of thin-film solar cells can be further improved.

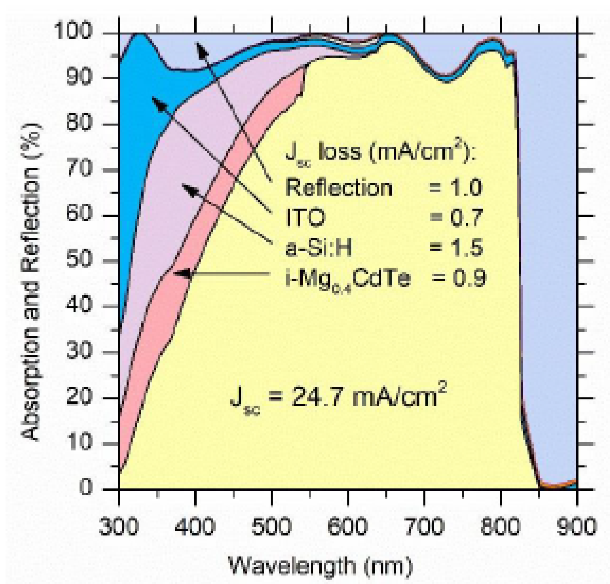

Figure 6. Simulated Absorptance Spectrum for CdTe Thin-film Solar Cells with a Calculated Photocurrent Density of 24.7 mA/cm^2 (The Simulated Device (structure A) has a 75-nm-thick SiO_2 Anti-reflection Coating Layer, a 55-nm-thick ITO Layer, an 8-nm-thick a-Si:H Hole-contact Layer and a 150-nm-thick Ag Back Contact.)

3.2 Optimize the novel lift-off technology using water-soluble MgTe sacrificial layers

The lift-off rate of the ELO thin films was studied by varying the MBE growth conditions and parameters including thickness and Cd composition in the Mg(Cd)Te sacrificial layer. The results are shown in Table . The lift-off time decreases dramatically as the MgTe thickness is increased from 5 nm to 28 nm. Incorporating dilute levels of Cd (1-8% mole fraction) increases the stability of the lift-off sample in air since MgTe is highly hygroscopic and reacts readily with moisture at the sample edge.

Table 2. MBE Growth Conditions and Parameters of MgTe Sacrificial Layer and Corresponding Lift-off Time for Samples with 5 mm × 5 mm Area

MgTe sacrificial layer growth condition	MgTe Thickness	Cd composition in MgTe sacrificial layer	Lift-off time (5 mm × 5 mm area)
Mg-rich	5 nm	0 %	> 30 min
	10 nm	0 %	> 30 min
	15 nm	0 %	> 30 min
	17 nm	0 %	> 20 min
	19 nm	0 %	20 min
Te-rich, soaking	20 nm	0 %	15 min
Te-rich	24 nm	0 %	10 min
	28 nm	8 %	> 15 min
		3 %	15 min
		2 %	10 min
		1 %	5 min
		0 %	3 min

4.0 RESULTS AND DISCUSSION

4.1 Proton radiation study of CdTe/MgCdTe DHs

The conventional CdTe DH samples shown in Fig. 7 are bombarded with stepwise 63-MeVprotons at fluences of 1.5×10^{11}, 3.75×10^{11}, 7.5×10^{11} and 1.5×10^{12} cm^{-2}, which are equivalent to ionizing doses of 20, 50, 100 and 200 kRad(Si) respectively. The samples are then characterized by steady-state PL, TRPL, and excitation intensity dependent PL. The laser wavelength is 532 nm.

Fig. 8 (a) and (b) show the steady-state PL and TRPL spectra of a set of the conventional CdTe/MgCdTe DH samples with varying doses of proton irradiation. The samples irradiated at 20, 50 and 100 kRad(Si) show increased PL intensity of 164%, 136%, 114% and increased PL decay time of 183%, 147%, 109%, respectively, compared to the reference sample without irradiation. The sample irradiated at 200 kRad(Si) shows a 12% decrease in PL intensity and 40% decrease in PL decay time. The PL peak intensity and the PL decay time of the samples are plotted together with the proton total ionizing dose in Fig. 8 (c). The nearly identical trends of the PL peak and the PL decay time indicate that the change in optical performance of the irradiated CdTe samples is mainly due to changes to the minority carrier lifetime. Increased minority carrier lifetime due to 68-MeV proton radiation doses up to 100 kRad(Si) could improve V_{oc} and power conversion efficiency. This interesting finding is attributed to the effect of the additional defects generated by proton radiation. Relatively low radiation defect densities can increase the localization and reduce the mobility of photogenerated carriers, thereby preventing them from reaching Shockley-Read-Hall (SRH) nonradiative recombination centers. Additionally, it is possible that the radiation defect energy levels are inside the conduction or valence band and thus do not act as SRH recombination centers. A similar effect has been observed in polycrystalline CdTe solar cells .

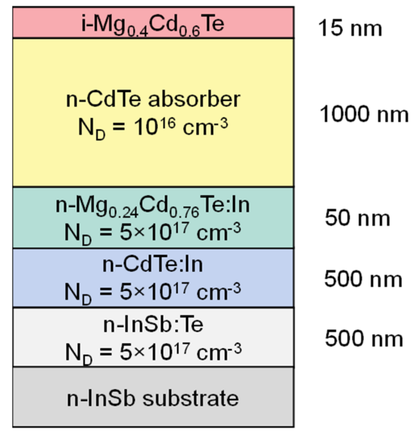

Fig. 7 Layer Structure of the Conventional CdTe/MgCdTe DH Design for Proton Radiation Test

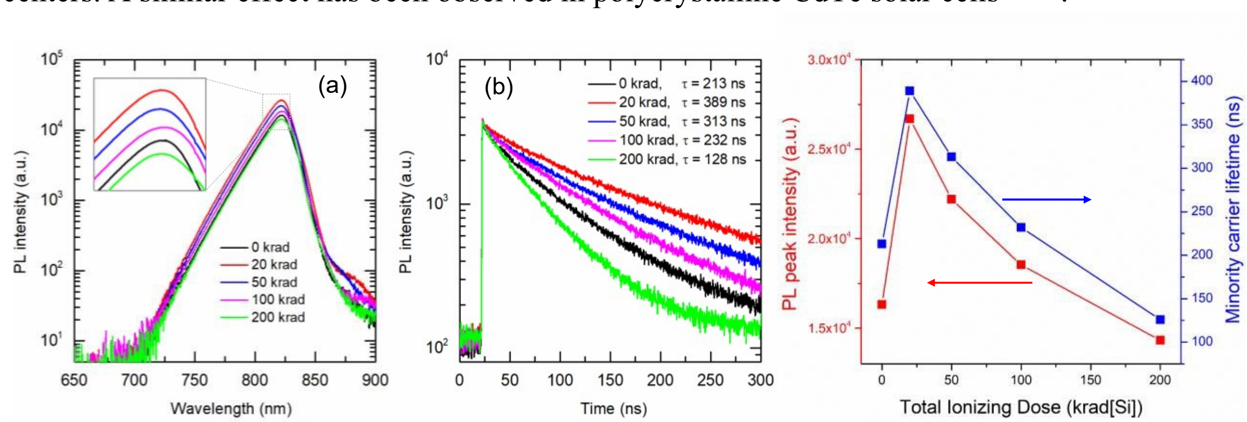

Fig. 8 (a) Steady-state PL and (b) TRPL Spectra of CdTe/MgCdTe DH Samples with Proton Irradiation Doses Ranging from 0-200 kRad (c) PL Peak Intensity and PL Decay Time of CdTe/MgCdTe DHs vs Proton Irradiation Dose

Excitation-density-dependent PL measurements are performed to study the defects generated by proton irradiation. Fig. 9 shows the PL spectra of CdTe/MgCdTe DH samples with 0, 20 and 200 kRad(Si) proton irradiation. The bandgap emission intensity in the PL spectra increases as the excitation intensity increases in all three samples. The irradiated samples exhibit sub-bandgap PL peaks in addition to the main emission peak from the bulk bandgap. These sub-bandgap emission peaks are not observed in the reference sample without irradiation. The sub-bandgap peaks gradually saturate with increasing excitation intensity, confirming that shallow defect energy levels are introduced by proton radiation. The sub-bandgap peaks shift to longer wavelengths with the increased irradiation dose, indicating that a higher radiation dose may introduce defects at deeper energy levels. No PL is observed at wavelengths longer than 1 m indicating there are few optically active deep levels in the CdTe absorber. The findings confirm that the CdTe/MgCdTe DH thin-film solar cells have superior proton radiation hardness and are suitable for space applications.

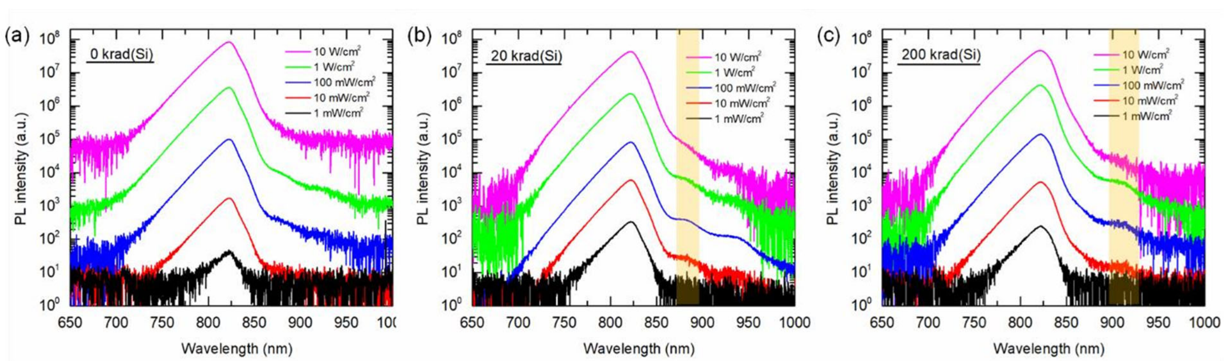

Figure 9. Excitation-density-dependant PL Spectra of CdTe/MgCdTe DH Samples with Ionizing Dose of (a) 0, (b) 20 and, (c) 200 kRad(Si) Proton Irradiation

Further studies of electrical properties of the CdTe DH devices as a function of proton irradiation are planned in March 2022.

4.2 Epitaxial lift-off CdTe/MgCdTe DHs for device applications

Indium bonding technology was used during the ELO process to form a conductive and adhesive layer between the CdTe lift-off samples and the superstrate, enabling the fabrication of thin film devices. Fig. 10 illustrates the processing steps. An 800 nm thick indium layer is deposited by thermal evaporation onto the bonding surfaces of both the polyimide film and the CdTe lift-off sample.

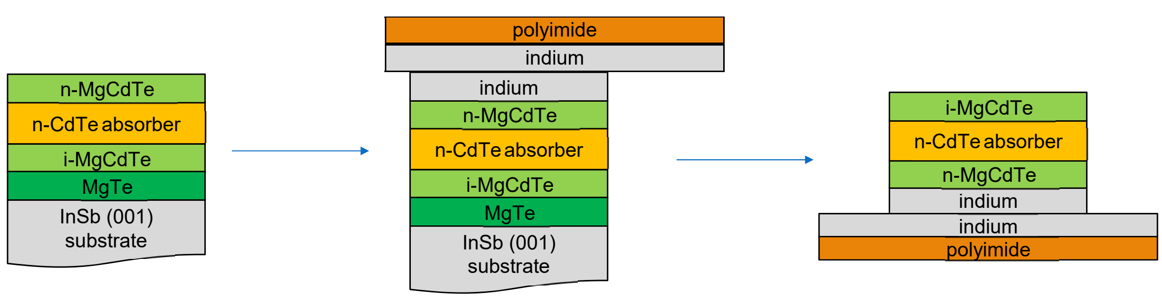

Figure 10. Schematic Flow Chart of the Processing Steps for the CdTeDH Thin Films Using Indium Bonding

After the indium deposition the lift-off sample and the polyimide film are brought into contact with mechanical pressure for 10 minutes followed by rapid thermal annealing at 150 ˚C for 10 minutes to form a tight bond between the lift-off sample and polyimide film. Then the sample and the superstrate are immersed into deionized (DI) water. Typically, the immersion process takes about 15 minutes to lift off a 1 cm × 1 cm thin film from the substrate in 55 ˚C DI water. Fig. 11 shows the PL spectra of the as-grown sample before ELO and the lift-off thin film with indium bonding layer. No significant PL degradation is observed across the sample area of the post-ELO film.

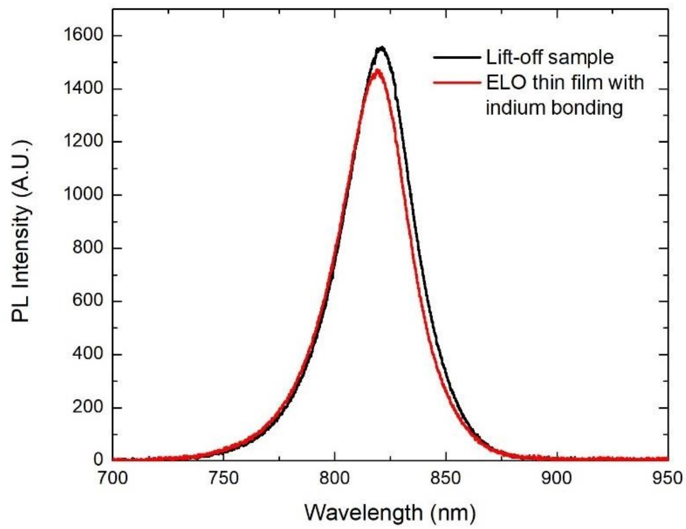

Figure 11. PL Spectra of the as-grown CdTeDH Lift-off Sample and the CdTe Lift-off Thin Film with Indium Bonding

A 75 nm thick ITO layer is deposited on the thin film after ELO to serve as a current spreading and contact layer. Fig. 12 shows the device structure and *J-V* characteristics. The fabricated monocrystalline CdTe thin-film solar cell demonstrates an efficiency of 9.8%. Further optimization of the ELO process is expected to improve the *FF* of future devices.

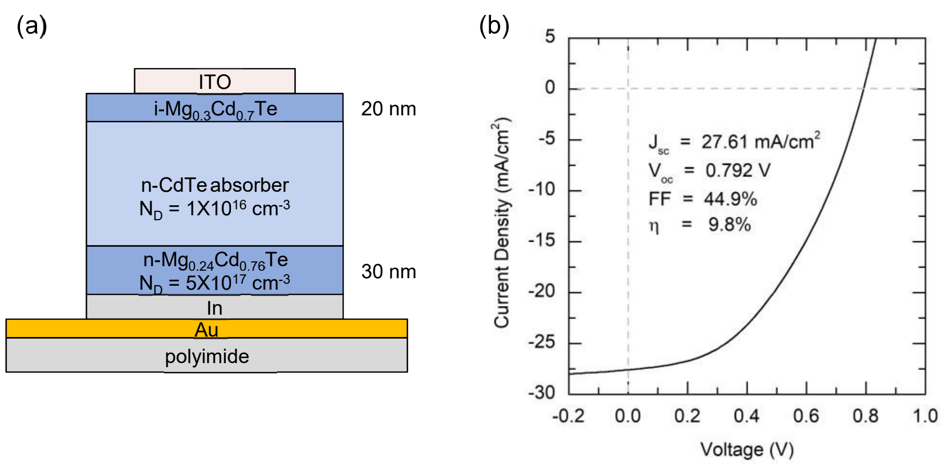

Figure 12. (a) Device Structure and (b) *J-V* Characteristics of the CdTe DH Thin-film Solar Cells

5.0 CONCLUSIONS

The material properties and radiation tolerance of CdTe/MgCdTe double heterostructures are evaluated before and after epitaxial lift-off from their substrates. Photoluminescence is observed to be enhanced after the double heterostructure is removed from the substrate. The lift-off process is optimized as a function of the structural composition and properties of the sacrificial etch layers. Photoluminescence is evaluated as a function of proton irradiation; the photoluminescence intensity is compared to the minority carrier lifetime evaluated from time-resolved photoluminescence, and the extent to which irradiation modifies the density of states below the bandgap is examined from the spectral shape of the photoluminescence.

REFERENCES

[1] B. Seredy ski, M. Król, P. Starzyk, R. Mirek, M. ciesiek, K. Sobczak, J. Borysiuk, D. Stephan, J.-G. Rousset, J. Szczytko, B. Pi tka, and W. Pacuski, Phys. Rev. Mat. **2**, 043406 (2018).

[2] C. M. Campbell, C.-Y. Tsai, J. Ding, T. T. McCarthy, B. Seredy ski, W. Pacuski, and Y.-H. Zhang, oral presentation in *45th IEEE Photovolt. Spec. Conf.*, Hawaii, United States, 10-15 June 2018.

[3] C. M. Campbell, C.-Y. Tsai, J. Ding, and Y.-H. Zhang, IEEE J. Photovoltaics **9**, 1834-1838 (2019).

[4] S. Liu, X.-H. Zhao, C. M. Campbell, M. B. Lassise, Y. Zhao, and Y.-H. Zhang, Appl. Phys. Lett. **107,** 041120 (2015).

[5] M. A. Green, Prog. Photovoltaic: Res. Appl. **20**, 472–476 (2012).

[6] M. Konagai, M. Sugimoto and K. Takahashi, J. Cryst. Growth **45**, 277 (1978).

[7] E. Yablonovitch, T. Gmitter, J. P. Harbison, and R. Bhat, Appl. Phys. Lett. **51**, 2222 (1987).

[8] A. Balocchi, A. Curran, T. C. M. Graham, C. Bradford, K. A. Prior, and R. J. Warburton, Appl. Phys. Lett. **86**, 011915 (2005)

[9] A. N. Tiwari, A. Romeo, D. Baetzner, and H. Zogg, Prog. Photovoltaics Res. Appl. **9**, 211 215 (2001).

[10] A. N. Tiwari, M. Krejci, F.-J. Haug, and H. Zogg, Prog. Photovoltaics Res. Appl. **7**, 393 397 (1999).

[6] D. J. Magginetti, J. A. Aguiar, J. R. Winger, M. A. Scarpulla, E. Pourshaban, and H. P. Yoon, Adv. Mater. Interfaces. **6**, 1900300 (2019).

[7] D. F. Marron, A. Meeder, S. Sadewasser, R. Wurz, C. A. Kaufmann, T. Glatzel, T. Schedel-Niedrig, and M. C. Lux-Steiner, J. Appl. Phys. **97**, 094915 (2005).

[8] D. L. McGott, M. D. Kempe, S. Glynn, N. Bosco, T. M. Barnes, N. M. Haegel, C. A. Wolden, and M. O. Reese, ACS Appl. Mater. Interfaces. **10**, 44854 (2018).

[9] S. M. Jovanovic, G. A. Devenyi, P. Kuyanov, J. L. Carvalho, K. Meinander, R. R. LaPierre, and J. S. Preston, Mater. Res. Express. **6**, 025913 (2019).

[14] W. Yang, J. Becker, S. Liu, Y.-S. Kuo, J.-J. Li, B. Landini, K. Campman, and Y.-H. Zhang, J. Appl. Phys. **115**, 203105 (2014).

[15] W. Yang, H. Yang, G. Qin, Z. Ma, J. Berggren, M. Hammar, R. Soref, and W. Zhou, Appl. Phys. Lett. **96**, 121107 (2010).

[16] S. J. Cho, D. Liu, J.-H. Seo, R. Dalmau, K. Kim, J. Park, J. Gong, D. Zhao, F. Wang, X. Yin, Y. H. Jung, I.-K. Lee, M. Kim, X. Wang, J. D. Albrecht, W. Zhou, B. Moody and Z. Ma, New J. Phys. **21**, 023011 (2019).

[17] Y. Zhao, M. Boccard, S. Liu, J. Becker, X.-H. Zhao, C. M. Campbell, E. Suarez, M. B. Lassise, Z. Holman, and Y.-H. Zhang, Nature Energy **1**, 16067 (2016).

[18] J. J. Becker, M. Boccard, C. M. Campbell, Y. Zhao, M. Lassise, Z. C. Holman, and Y.-H. Zhang, IEEE J. Photovoltaics **7**, 900–905 (2017).

[19] X.-H. Zhao, S. Liu, C. M. Campbell, Y. Zhao, M. B. Lassise, and Y.-H. Zhang, IEEE J. Photovoltaics **7**, 913–918 (2017).

[20] J. Ding, and Y.-H. Zhang, in *Proc. 46th IEEE Photovolt. Spec. Conf.*, Chicago, United States, 1621 June 2019, pp. 21-24.

[21] M. J. DiNezza, X.-H. Zhao, S. Liu, A. P. Kirk, and Y.-H. Zhang, Appl. Phys. Lett. **103**, 193901 (2013).

[22] Y. Zhao, X.-H. Zhao, and Y.-H. Zhang, IEEE J. Photovoltaics **7**, 690-694 (2017).

[23] U. Rau, Phys. Rev. B **76**, 085303 (2007).

[24] O. D. Miller, E. Yablonovitch, and S. R. Kurtz, IEEE J. Photovoltaics **2**, 303-311 (2012).

[25] D. Ding, S. R. Johnson, S.-Q. Yu, S.-N. Wu, and Y.-H. Zhang, J. Appl. Phys. **110**, 123104 (2011).

[26] S. Liu, D. Ding, S. R. Johnson, and Y.-H. Zhang, in *Proc. SPIE 8256, Physics, Simulation, and Photonic Engineering of Photovoltaic Devices*, San Francisco, United States, 21 February 2012, 82560M.

[27] D. L. Batzner, A. Romeo, M. Terheggenb, M. Dobeli, H. Zogg, and A. N. Tiwari, Thin Solid Films 451-452 (2004) 536–543

PUBLICATIONS AND PRESENTATIONS

Journal and Proceeding

1. J. Ding, C. M. Campbell, J. J. Becker, C.-Y. Tsai, S. T. Schaefer, T. T. McCarthy, M. Boccard, Z. C. Holman and Y.-H. Zhang, "Monocrystalline 1.7-eV MgCdTe solar cells", *J. Appl. Phys.* 131, 023107 (2022).
   Editor's Pick
2. J. Ding, C.-Y. Tsai, Z. Ju and Y.-H. Zhang, "Epitaxial lift-off CdTe/MgCdTe double heterostructures for thin-film and flexible solar cells applications", *Appl. Phys. Lett*. 118, 181101 (2021). Editor's Pick / Feature & Selected as "Scilight" in AIP.
3. J. Ding, X. Qi, Y. Zhao, and Y.-H. Zhang, "Epitaxial lift-off monocrystalline CdTe/MgCdTe double heterostructures and proton radiation study for space applications", *IEEE Photovoltaic Specialists Conference* (2021) pp. 1213-1216.

Conference Presentation (Selected)

1. Jia Ding, Preston T. Webster, Xin Qi and Yong-Hang Zhang "Epitaxial lift-off monocrystalline CdTe/MgCdTe double heterostructures and proton radiation study for space applications", 21st International Conference in Molecular Beam Epitaxy, Puerto Vallarta, Mexico (2021).
2. Jia Ding, Xin. Qi, Yuji. Zhao, and Yong-Hang Zhang, "Epitaxial lift-off monocrystalline CdTe/MgCdTe double heterostructures and proton radiation study for space applications", 48th IEEE Photovoltaic Specialist Conference, Miami, FL, USA (2021).

Conference Presentation (Submitted)

1. Xin Qi, Jia Ding, Zheng Ju, Stephen Schaefer, and Yong-Hang Zhang, "Flexible CdTe/MgCdTe Double-Heterostructure Solar Cells Made of Epitaxial Lift-off Thin Film", 49th IEEE Photovoltaic Specialist Conference, Philadelphia, PA, USA (2022).

DISTRIBUTION LIST

DTIC/OCP 8725 John J. Kingman Rd, Suite 0944 Ft Belvoir, VA 22060-6218	1 cy
AFRL/RVIL Kirtland AFB, NM 87117-5776	1 cy
Official Record Copy AFRL/RVS/Preston Webster	1 cy

(This Page Intentionally Left Blank)